24th INTERNATIONAL CONGRESS ON SOUND AND VIBRATION
23–27 July 2017, London

APPLICATION OF THE LOCAL PLANE WAVE METHOD TO MEASURE IN-SITU SOUND ABSORPTION USING A SPHERICAL MICROPHONE ARRAY

Niels Consten
SoundInsight BV, Hengelosestraat 500, 7521 AN Enschede, The Netherlands.
email: n.consten@soundinsight.nl

Anne de Jong
SoundInsight BV, Hengelosestraat 500, 7521 AN Enschede, The Netherlands.

Ysbrand Wijnant
SoundInsight BV, Hengelosestraat 500, 7521 AN Enschede, The Netherlands;
University of Twente, Drienerlolaan 5, 7500 AE Enschede, The Netherlands.

Former studies have shown that the Local Plane Wave (LPW) method can be used to measure the (effective) in-situ sound absorption coefficient of any surface. The LPW-method is based on a local plane wave assumption, in which the normal component of the sound field in each spatial coordinate is approximated by an incident and a reflected plane wave. This is contrary to conventional methods that rely on a known global sound field, like the impedance tube (plane wave) and reverberation room (diffuse field) methods. The LPW-method can therefore be applied in sound fields for which a model is not available. This has been numerically and experimentally validated using a probe consisting of 8 MEMS-microphones in an open cubical structure.
In this paper, the LPW-method will be applied to a rigid spherical microphone array. The well-known plane wave expansion in spherical harmonics will be used to formulate a local model of the sound field in the presence of a rigid sphere. The resulting model will be used to infer the sound field for the case the rigid sphere would not be present. The (effective) in-situ sound absorption coefficient is then computed from the parameters of this inferred sound field. Using numerical and experimental results, the validity and usefulness of the LPW-method to measure sound absorption using a spherical microphone array will then be shown.

Keywords: absorption, in-situ, LPW, spherical array, SonoCat

1. Introduction

Former studies have shown that the Local Plane Wave (LPW) method can be used to measure the (effective) in-situ sound absorption coefficient of a material/surface in an a-priori unknown sound field [1, 2, 3, 4]. The LPW-method is based on a local plane wave assumption, in which the normal component of the sound field in each spatial coordinate is approximated by an incident and a reflected plane wave. This allows acousticians to estimate the incident sound intensity in unknown sound fields such that they can assess the efficiency of absorption material in its application. This is contrary to conventional laboratory methods that rely on a known global sound field, like the impedance tube (plane wave) [5, 6] and reverberation room (diffuse field) [7] methods.

The theory and applicability of the LPW-method has been widely investigated for pu- and pp-probes. It has also been numerically and experimentally validated using a probe consisting of 8

MEMS-microphones in an open cubical structure. This paper aims to apply the LPW-method to a rigid spherical microphone array as these type of microphone arrays have been introduced in the acoustic industry over the past few years. The theory of the LPW-method applied to spherical microphone arrays is presented in Section 2. This will be validated both numerically and experimentally in Section 3. Finally, conclusions will be drawn in Section 4.

2. Theory

2.1 Sound absorption coefficient

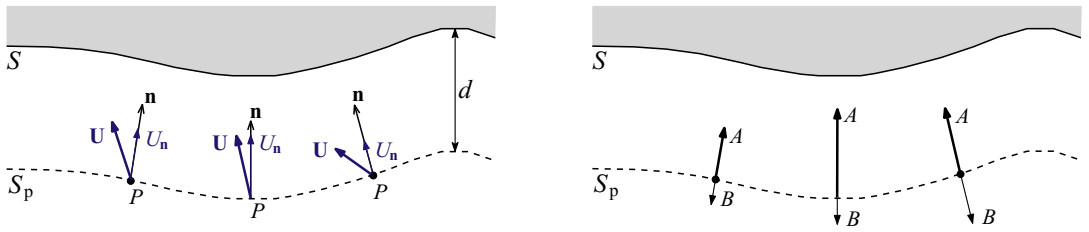

(a) Real sound field. (b) Approximated sound field using LPW-method.

Figure 1: Sound field in front of a material surface S. Taken from [8].

The sound absorption coefficient of a surface is defined as the ratio of the active (net) sound power and the incident sound power:

$$\alpha = \frac{W_{\mathrm{ac}}}{W_{\mathrm{in}}}, \tag{1}$$

with W_{ac} and W_{in} the active and incident sound power respectively. Both powers can be calculated by integrating their associated intensities over the surface:

$$W_{\mathrm{ac}} = \int_{S_{\mathrm{p}}} \mathbf{I}_{\mathrm{ac}} \cdot \mathbf{n}\, \mathrm{d}S, \tag{2}$$

$$W_{\mathrm{in}} = \int_{S_{\mathrm{p}}} \mathbf{I}_{\mathrm{in}} \cdot \mathbf{n}\, \mathrm{d}S, \tag{3}$$

where $\mathbf{I}_{\mathrm{ac}} = \frac{1}{2}\Re\big(P\overline{\mathbf{U}}\big)$ is the active (net) sound intensity vector with P the complex sound pressure and $\overline{\mathbf{U}}$ the conjugate of the complex particle velocity vector, and $\mathbf{n}$ is the vector pointing normal into the surface S_{p}, as shown in Fig. 1a. $\mathbf{I}_{\mathrm{in}}$ is the incident sound intensity vector, being equal to the active sound intensity vector for a fully absorbing surface. The active sound intensity vector in the direction normal to the surface can easily be measured with any pu- or pp-probe. However, determination of the incident sound intensity vector in an unknown sound field is not possible. A way of estimating the normal component of the incident sound intensity vector is by using the so-called *local plane wave* (LPW) method, which will be explained in next subsection.

2.2 Theory of the LPW-method

The LPW-method is based on a local plane wave assumption, in which the normal component of the sound field in each spatial coordinate is approximated by an incident and a reflected plane wave as shown in Fig. 1b. Using the $e^{i\omega t}$-convention, i.e. $p(\mathbf{r},t) = \Re\left\{P\left(\mathbf{r},\omega\right)e^{i\omega t}\right\}$, the complex sound pressure P and complex particle velocity in normal direction $U_{\mathrm{n}} = \mathbf{U}\cdot\mathbf{n}$ can be written as [8]:

$$P\left(\mathbf{r},k\right) = A\left(\mathbf{r},k\right) + B\left(\mathbf{r},k\right), \tag{4}$$

$$U_{\mathrm{n}}\left(\mathbf{r},k\right) = \frac{A\left(\mathbf{r},k\right)}{\rho_0 c_0} - \frac{B\left(\mathbf{r},k\right)}{\rho_0 c_0} \tag{5}$$

where $\mathbf{r}$ is the position vector, $k = \omega/c_0$ is the wave number, A and B are the complex amplitudes of the incident and reflected waves respectively and $\rho_0 c_0$ is the characteristic impedance. Note that we have omitted the e^{-ikz}- and e^{ikz}-exponentials by choosing $z = 0$ where z is a *local* coordinate axis aligned with the normal vector $\mathbf{n}(\mathbf{r})$. From this assumption it follows that the normal incident and reflected intensity are:

$$\mathbf{I}_{\text{in}}(\mathbf{r}, k) \cdot \mathbf{n}(\mathbf{r}) \overset{\text{LPW}}{=} \frac{|A(\mathbf{r}, k)|^2}{2\rho_0 c_0}, \tag{6}$$

$$\mathbf{I}_{\text{refl}}(\mathbf{r}, k) \cdot \mathbf{n}(\mathbf{r}) \overset{\text{LPW}}{=} \frac{|B(\mathbf{r}, k)|^2}{2\rho_0 c_0}. \tag{7}$$

Furthermore, the active intensity in normal direction can also be written in terms of A and B:

$$\mathbf{I}_{\text{ac}}(\mathbf{r}, k) \cdot \mathbf{n}(\mathbf{r}) \overset{\text{LPW}}{=} \frac{|A(\mathbf{r}, k)|^2}{2\rho_0 c_0} - \frac{|B(\mathbf{r}, k)|^2}{2\rho_0 c_0}, \tag{8}$$

such that the active intensity in normal direction is equal to the incident intensity in normal direction minus the reflected intensity in normal direction. Hence, if one can determine A and B, one can find the incident and active intensities by evaluating Eqs. (6) and (8), and calculate the sound absorption coefficient according to Eqs. (1), (2) and (3). Using a pu-probe, one can solve Eqs. (4) and (5) for A and B easily. Determination of A and B using a 1D and 3D pp-probe is elaborated in next subsection.

2.3 Formulation for a 1D and 3D pp-probe

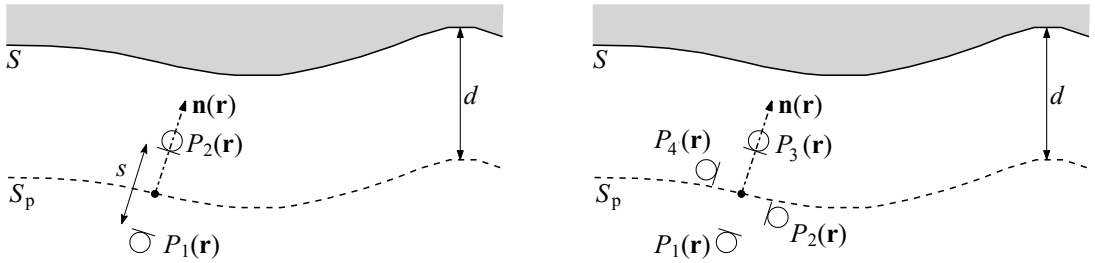

(a) 1D (b) 3D

Figure 2: Different pp-probes. Taken and modified from [8].

1D and 3D pp-probes (see Fig. 2) are generally used to determine the (normal component of) the active sound intensity vector using the well-known finite difference method. The estimated sound pressure and particle velocity at the middle point of the probe can be used to apply the LPW-method as explained in Section 2.2. However, a different (more intuitive) formulation can also be derived. For a 1D pp-probe with two microphones a distance s apart (see Fig. 2a), the LPW-method can be written as [8]:

$$P_1(\mathbf{r}, k) = A(\mathbf{r}, k)\, e^{-iks/2} + B(\mathbf{r}, k)\, e^{iks/2}, \tag{9}$$

$$P_2(\mathbf{r}, k) = A(\mathbf{r}, k)\, e^{iks/2} + B(\mathbf{r}, k)\, e^{-iks/2}, \tag{10}$$

where P_1 and P_2 are the measured microphone pressures. Solving above equations for A and B enables determination of the sound absorption coefficient according to the procedure prescribed at the end of Section 2.2. For a 3D pp-probe (see for example Fig. 2b) the following set of linear equations should be solved:

$$\mathbf{p}(\mathbf{r}, k) = \mathbf{H} \cdot \mathbf{a}(\mathbf{r}, k) \tag{11}$$

with

$$\mathbf{p}\left(\mathbf{r},k\right)=\begin{Bmatrix}P_1\left(\mathbf{r},k\right)\\ \vdots\\ P_M\left(\mathbf{r},k\right)\end{Bmatrix},\quad \mathbf{H}=\begin{bmatrix}e^{-ikz_1} & e^{ikz_1}\\ \vdots & \vdots\\ e^{-ikz_M} & e^{ikz_M}\end{bmatrix},\quad \mathbf{a}\left(\mathbf{r},k\right)=\begin{Bmatrix}A\left(\mathbf{r},k\right)\\ B\left(\mathbf{r},k\right)\end{Bmatrix}, \tag{12}$$

where $P_1 \dots P_M$ are the measured microphone pressures at positions $z = z_1 \dots z_M$ and $M \geq 4$ is the number of microphones. Recall that z is the *local* coordinate axis aligned with the normal vector $\mathbf{n}\left(\mathbf{r}\right)$ with $z = 0$ at $\mathbf{r}$. Solving the linear set of equation for $\mathbf{a}$ in a least-squares sense yields:

$$\mathbf{a}_{\text{ls}}\left(\mathbf{r},k\right)=\mathbf{H}^{+}\cdot\mathbf{p}\left(\mathbf{r},k\right), \tag{13}$$

with

$$\mathbf{H}^{+}=\left(\mathbf{H}^{\text{H}}\mathbf{H}\right)^{-1}\mathbf{H}^{\text{H}}, \tag{14}$$

where $^{\text{H}}$ denotes the conjugate transpose (or Hermitian conjugate). A least squares solution minimizes the sum of the squared residuals of the microphone signals. These residuals can be measurement noise, which encourages the use of multiple microphones. Solving Eq. (13) for A and B enables determination of the sound absorption coefficient according to the procedure prescribed at the end of Section 2.2.

2.4 Including scattering of a rigid sphere probe

The well-known plane wave expansion in spherical harmonics will be used to formulate a local model of the sound field in the presence of a rigid sphere. A plane wave in spherical waves is defined as [9]:

$$P_{\text{in}}\left(\mathbf{r},\mathbf{k}\right)=\tilde{A}\left(\mathbf{k}\right)e^{i\mathbf{k}\cdot\mathbf{r}}=\tilde{A}\left(\mathbf{k}\right)\sum_{n=0}^{\infty}i^n\left(2n+1\right)j_n\left(kr\right)P_n\left(\frac{\mathbf{k}\cdot\mathbf{r}}{kr}\right), \tag{15}$$

where $\mathbf{r}$ is the position vector of length r, $\mathbf{k}$ is the wave vector of length k, $\tilde{A}$ is the complex amplitude of the plane wave, j_n is the spherical Bessel function of order n and P_n is the Legendre polynomial of degree n. The scattered field around a rigid sphere can be represented by spherical waves emanating from the surface of the sphere and is therefore described as:

$$P_{\text{sc}}\left(\mathbf{r},\mathbf{k}\right)=\sum_{n=0}^{\infty}C_n\left(\mathbf{k}\right)h_n^{(2)}\left(kr\right)P_n\left(\frac{\mathbf{k}\cdot\mathbf{r}}{kr}\right), \tag{16}$$

where C_n is a constant determined by the impinging sound waves and $h_n^{(2)}$ is the Hankel function of the second kind of order n. Considering a rigid sphere with radius a and center at $r = 0$, the radial component of the particle velocity at $r = a$ should be zero. Determination of constant C_n is hence obtained after employment of the following boundary condition:

$$\frac{\partial}{\partial r}\left(P_{\text{in}}\left(\mathbf{r},\mathbf{k}\right)+P_{\text{sc}}\left(\mathbf{r},\mathbf{k}\right)\right)\Big|_{r=a}=0. \tag{17}$$

Substitution of Eqs. (15) and (16) into Eq. (17) yields that

$$C_n\left(\mathbf{k}\right)=-\tilde{A}\left(\mathbf{k}\right)i^n\left(2n+1\right)\frac{j_n^{'}\left(ka\right)}{h_n^{(2)'}\left(ka\right)}, \tag{18}$$

where the apostrophes denote the derivatives of the spherical Bessel and Hankel functions. Hence the total sound field $P_{\text{tot}} = P_{\text{in}} + P_{\text{sc}}$ becomes:

$$P_{\text{tot}}\left(\mathbf{r},\mathbf{k}\right)=\tilde{A}\left(\mathbf{k}\right)\left(e^{i\mathbf{k}\cdot\mathbf{r}}-\sum_{n=0}^{\infty}i^n\left(2n+1\right)\frac{j_n^{'}\left(ka\right)}{h_n^{(2)'}\left(ka\right)}h_n^{(2)}\left(kr\right)P_n\left(\frac{\mathbf{k}\cdot\mathbf{r}}{kr}\right)\right). \tag{19}$$

If we now consider two plane waves with wave vectors $\mathbf{k}_A = [0, 0, -k]$ and $\mathbf{k}_B = [0, 0, k]$ (which is in accordance with the LPW-method) and evaluate them at the m'th microphone position $\mathbf{r}_m$ on the sphere with radius a, then the transfer matrix in Section 2.3 becomes:

$$\mathbf{H} = \begin{bmatrix} H_{1A} & H_{1B} \\ \vdots & \vdots \\ H_{MA} & H_{MB} \end{bmatrix}, \tag{20}$$

where

$$H_{mA} = e^{i\mathbf{k}_A \cdot \mathbf{r}_m} - \sum_{n=0}^{\infty} i^n \left(2n+1\right) \frac{j_n^{'}\left(ka\right)}{h_n^{(2)'}\left(ka\right)} h_n^{(2)}\left(ka\right) P_n\left(\frac{\mathbf{k}_A \cdot \mathbf{r}_m}{ka}\right), \tag{21}$$

$$H_{mB} = e^{i\mathbf{k}_B \cdot \mathbf{r}_m} - \sum_{n=0}^{\infty} i^n \left(2n+1\right) \frac{j_n^{'}\left(ka\right)}{h_n^{(2)'}\left(ka\right)} h_n^{(2)}\left(ka\right) P_n\left(\frac{\mathbf{k}_B \cdot \mathbf{r}_m}{ka}\right). \tag{22}$$

Solving Eq. (13) for A and B with $\mathbf{H}$ as in Eq. (20) enables determination of the sound absorption coefficient according to the procedure prescribed at the end of Section 2.2. By inferring the sound field for the case the rigid sphere would not be present, the LPW-method can thus be applied to measure sound absorption using a spherical microphone array.

3. Validation

The validity and usefulness of this measurement procedure for sound absorption is shown in this section. For that purpose, use is made of SonoCat, a rigid spherical microphone array consisting of 8 digital MEMS-microphones, see Fig. 5b. The spherical coordinates of the microphones, as shown in Table 1, are (semi-)equidistantly distributed and the $\theta = 180°$ direction is aligned with the normal surface vector. Both numerical simulations and experimental measurements are performed for a normal incident plane wave and the results will be presented in next subsections.

Table 1: Microphone positions at the rigid sphere with the sphere center at $r = 0$

Mic	Radial distance r $[mm]$	Polar angle θ [°]	Azimuthal angle ϕ [°]
1	15	22.3	180.0
2	15	50.8	0.0
3	15	85.0	12.4
4	15	85.0	-12.4
5	15	95.0	56.3
6	15	12.9	180.0
7	15	95.0	-56.3
8	15	15.8	0.0

3.1 Numerical simulations

The response of a rigid sphere with a radius of 15mm in front of an impedance surface is simulated in a finite element analysis, see Fig. 3. A background pressure field consisting of a plane wave travelling in the $\mathbf{n}$-direction and an opposite travelling plane wave (with a reflection coefficient in accordance with the impedance boundary conditions) is set. A Sommerfeld radiation condition is applied at the domain boundary and the mesh size is chosen sufficiently small. The scattering problem

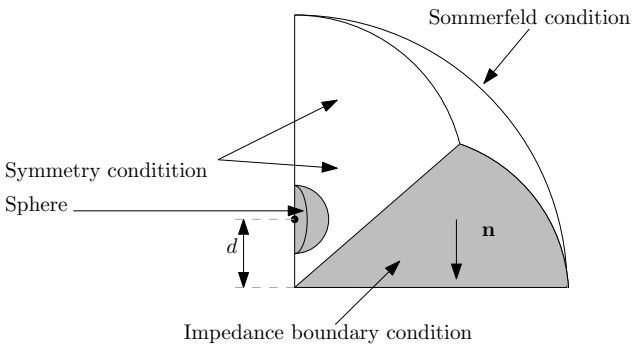

Figure 3: Symmetric simulation model

is solved and the total pressure field is evaluated at the same positions as SonoCat's microphone positions. Note that for normal incidence sound waves there is no azimuthal angle dependency, such that an axisymmetric model could have been used. The sound absorption coefficient is then calculated according to the procedure in Sections 2.3 and 2.4.

Three different normal impedance surfaces are considered, i.e. $Z_n = \rho_0 c_0$, $Z_n = (1+2i)\,\rho_0 c_0$ and $Z_n = \infty$, such that an absorption coefficient of $\alpha = 1$, $\alpha = 0.5$ and $\alpha = 0$ is to be expected, respectively. The distance of the sphere center to the surface is also investigated for $d = 3.0$ cm, $d = 4.5$ cm and $d = 6.0$ cm. The results of these simulations are presented in Fig. 4 for several $1/3$'th octave band frequencies.

Up to 1kHz the sound absorption curves follow the expected values very well for all impedance surfaces and sphere-surface distances. At frequencies above 1kHz this is also true for an impedance surface $Z_n = \rho_0 c_0$ (expectation: $\alpha = 1$). For the other impedance surfaces, deviations from the expected values start to occur for increasing frequencies. These deviations are less for impedance surface $Z_n = (1+2i)\,\rho_0 c_0$ (starting from 2kHz, expectation: $\alpha = 0.5$) compared to $Z_n = \infty$ (starting from 1kHz, expectation: $\alpha = 0$).

For a certain surface impedance Z_n (except for $Z_n = \rho_0 c_0$), the sphere-surface distance influences the deviations. In general, the smaller the sphere-surface distance, the more deviations in the sound absorption values for increasing frequencies.

These (small) deviations can be explained by the fact that the applied model does not account for the surface reflection of the scattered waves from the sphere. For higher frequencies, more scattering of the sphere occurs which will reflect on the impedance surface if the absorption is low. These scattering reflections decrease over the distance, such that a larger sphere-surface distance is preferred in this situation.

Hence, for very well absorbing surfaces, the LPW-method performs very well for normal incident plane waves independent on the sphere-surface distance. For less absorbing surfaces, the performance is also fine but the deviations depend on the frequency and the sphere-surface distance. In general, the more reflective the surface and the smaller the sphere-surface distance, the more deviations are seen in the sound absorption coefficient for increasing frequencies. However, most absorbers comprise good absorptive properties at high frequencies and less at lower frequencies, such that the LPW-method can be applied in many applications using a spherical microphone array.

3.2 Experimental results

The normal incident sound absorption coefficients of two melamine resin foam samples with a different thickness (5 and 10 cm) is measured with both SonoCat and an impedance tube at the University of Twente. The impedance tube measurements were performed according to ISO 10534-2:2008 [6]. The SonoCat measurements were performed in a room with anechoic properties above 300 Hz to avoid unwanted reflections, see Fig. 5. A plywood plate with a thickness of approximately 1.5 cm is used as the backing material and the sphere-surface distance d is approximately 3 cm. A

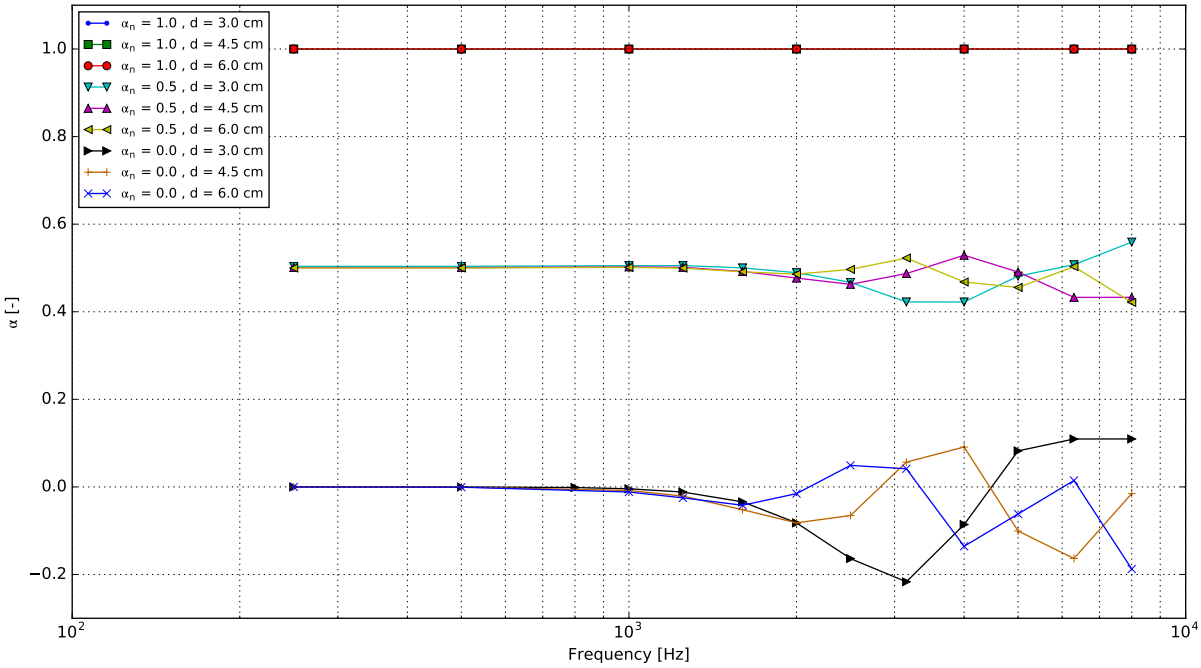

Figure 4: Sound absorption for normal incidence

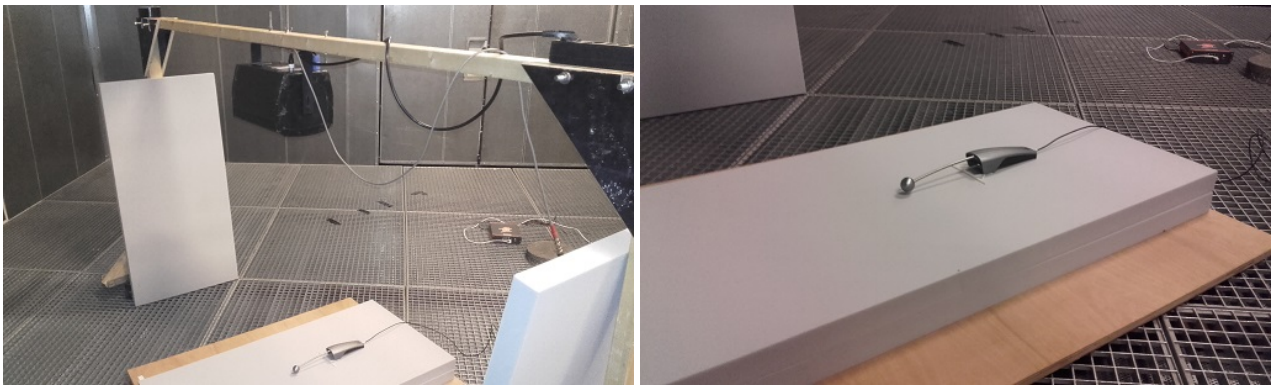

(a) Setup (b) Zoom

Figure 5: SonoCat measurement

single cone speaker is positioned at a height of approximately 1.5 m above the SonoCat emitting a broadband white-noise sound. It is assumed that the speaker is sufficiently far away from the surface such that the emitted sound waves have become plane waves above 300 Hz.

The results of the measurements are shown in Fig. 6 together with the material specifications as provided by the manufacturer. In overall, a good match is achieved between all absorption curves for each material thickness. Differences occur between all curves, even for the impedance tube measurements, but they are small. The general trends are in comparison for each curve. For example, the 'dip' around 3 kHz in Fig. 6a appears in all three curves. This shows that the LPW-method can be used to measure sound absorption of a surface with a rigid spherical microphone array.

4. Conclusion

The LPW-method to measure the (effective) in-situ sound absorption coefficient using a spherical microphone array has been presented in this paper. The model for spherical microphone arrays infers the sound field for the case the rigid sphere would not be present by adding the scattering of a plane

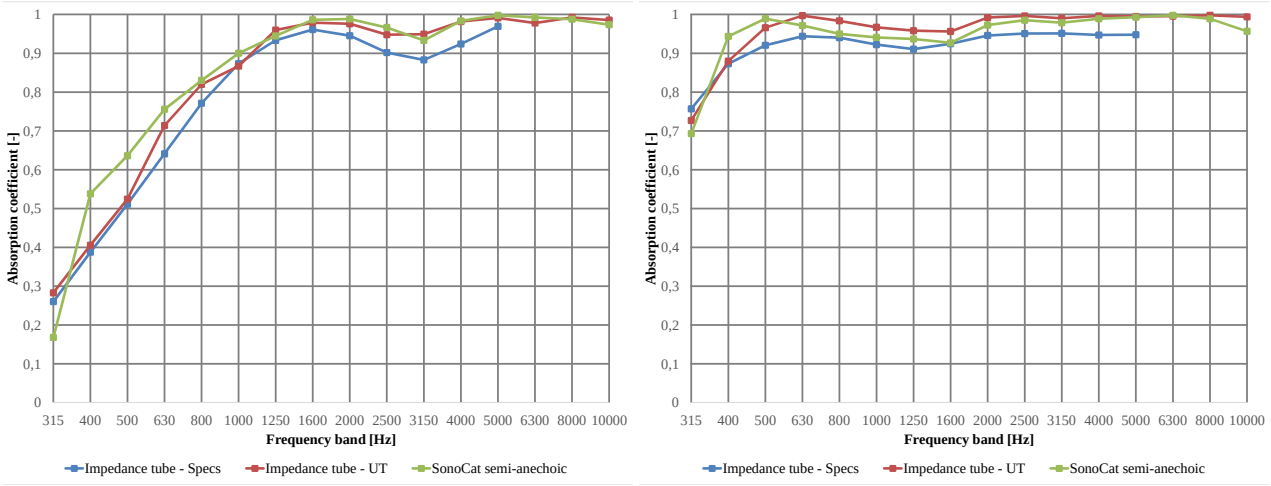

(a) 50mm thickness.

(b) 100mm thickness.

Figure 6: Sound absorption of a melamine foam for normal incidence: Impedance tube vs SonoCat

wave around a rigid sphere to the model. The validity and usefulness of the model has been proven numerically and experimentally for a normal incident plane wave. Considering previous studies on the LPW-method, it is to be expected that the LPW-method applied to a spherical microphone array will also be useful in other sound fields. It can therefore be concluded that a rigid spherical microphone array can be used to measure the (effective) in-situ sound absorption coefficient of a surface/material.

REFERENCES

1. Wijnant, Y.H., Kuipers, E.R. and de Boer, A., Development and application of a new method for the in-situ measurement of sound absorption, *Proceedings of the 24th ISMA*, Leuven, Belgium, 20–22 September, (2010).

2. Kuipers, E.R., Wijnant, Y.H. and de Boer, A., Theory and application of a new method for the in-situ measurement of sound absorption, *Proceedings of the 37th DAGA*, Düsseldorf, Germany, 21–24 March, (2011).

3. Kuipers, E.R., Wijnant, Y.H. and de Boer, A., A numerical study of a method for measuring the effective in situ sound absorption coefficient, *Journal of the Acoustical Society of America*, **132** (3), 236–242, (2012).

4. Wijnant, Y.H., On the local plane wave methods for in situ measurement of acoustic absorption, *Proceedings of the 21th ICSV*, Beijing China, 13–17 March, (2014).

5. ISO 10534-1:1996: Acoustics - Determination of sound absorption coefficient and impedance in impedance tubes - Part 1: Method using standing wave ratio, (1996).

6. ISO 10534-2:1998: Acoustics - Determination of sound absorption coefficient and impedance in impedance tubes - Part 2: Transfer-function method, (1998).

7. ISO 354:2003: Acoustics - Measurement of sound absorption in a reverberation room, (2003).

8. Kuipers, E.R., Wijnant, Y.H. and de Boer, A., Measuring Sound Absorption: Considerations on the Measurement of the Active Acoustic Power, *Acta Acustica united with Acustica*, **100**, 193–204, (2014).

9. Williams E.G., *Fourier Acoustics, Sound Radiation and Nearfield Acoustical Holography*, Academic Press, first edition, (2007).